

A new method for remote sensing of moisture profiles in the arable layer at three frequencies; experimental case study

Konstantin Muzalevskiy

To cite this article: Konstantin Muzalevskiy (2021) A new method for remote sensing of moisture profiles in the arable layer at three frequencies; experimental case study, International Journal of Remote Sensing, 42:7, 2377-2390, DOI: [10.1080/01431161.2020.1851795](https://doi.org/10.1080/01431161.2020.1851795)

To link to this article: <https://doi.org/10.1080/01431161.2020.1851795>



Published online: 24 Dec 2020.



Submit your article to this journal [↗](#)



Article views: 106



View related articles [↗](#)



View Crossmark data [↗](#)



A new method for remote sensing of moisture profiles in the arable layer at three frequencies; experimental case study

Konstantin Muzalevskiy

Laboratory of Radiophysics of the Earth Remote Sensing, Kirensky Institute of Physics Federal Research Center KSC Siberian Branch Russian Academy of Sciences, Krasnoyarsk, Russian Federation

ABSTRACT

In this paper, the possibilities of remote sensing of moisture profiles in the arable layer were theoretically and experimentally studied based on the nadir measurements of reflection coefficients at three frequencies of 1.26 GHz, 796 MHz and 641 MHz. The reflection coefficients were measured by the impulse method during natural cycles of evaporation and moistening of an arable layer at the agricultural field being under steam, located at 56°05'N, 92°40' E in the area of the Minino village, Krasnoyarsk region, the Russian Federation. The soil moisture profiles were retrieved in the course of solving the inverse problem, in which the reflection coefficients at different frequencies acted as an informative sign. The root-mean-square error and the determination coefficient (R^2) between retrieved and measured moisture values in the topsoil thickness of 0.15 m were 3.3% and 0.79, respectively. In the course of theoretical calculations, it was shown that in practice, it is impossible to predict the sensing depth of the arable layer without preliminary information on the form of moisture profile. Moreover, the sensing depth depends not only on the form of soil moisture profile but also on frequency. In this regard, it is impossible to correlate the effective soil moisture, retrieved from single-frequency measurements of the reflection coefficient in the approximation of homogeneous topsoil, with the specific thickness of topsoil. The study shows the promise of developing multi-frequency radar systems for remote sensing of soil moisture profiles in the arable layer, the potential of which can be realized on lightweight unmanned area vehicle (UAV) platforms.

ARTICLE HISTORY

Received 24 April 2020
Accepted 30 September 2020

Keywords

microwave remote sensing;
radar; UAV; soil moisture
profile; soil permittivity

1. Introduction

In recent years, the improvement of precision farming methods associated (Candiago et al. 2015) with the widespread introduction of technologies for remote monitoring of the condition of agricultural fields and crops using unmanned aerial vehicles (UAV). These technologies use multispectral observations in the infrared and visible bands (Haboudane et al. 2004) to quantify the seasonal variation of crops photosynthesis (normalized difference vegetation index), the water content in plant leaves (normalized difference

CONTACT Konstantin Muzalevskiy  rsdkm@ksc.krasn.ru  Laboratory of Radiophysics of the Earth Remote Sensing, Kirensky Institute of Physics Federal Research Center KSC Siberian Branch Russian Academy of Sciences, Krasnoyarsk, Russian Federation

water index), nitrogen consumption by plants (green normalized difference water index), etc. At the same time, until now, the technologies of soil moisture remote sensing from UAV platforms have not been introduced into the precision farming methods of individual farms. However, the success of crops cultivation is mostly determined by the content in root-zone of the necessary amount of productive moisture during the growing season. Direct measurements of the vertical distribution of moisture in the arable layer using optical multispectral observations are hindered by the impossibility of waves in infrared and visible bands penetrating through vegetation cover into the soil. Over the past 40 years, many studies (Entekhabi et al. 2014; Ulaby and Long 2015; Shutko 1982; Schmugge 1978) have successfully demonstrated the use of microwave radar and radiometric methods for remote sensing of soil moisture in the microwave band (above 1 GHz). In this frequency range, the sensing depth of topsoil moisture is no more than 5 cm (Entekhabi et al. 2014). It fundamentally does not allow to retrieve moisture distribution in the arable layer (up to about 0.3 m). The moisture distribution in the arable layer can be fundamentally retrieved with using the decimetre wavelength band (about 0.7 m wavelength) (Sadeghi et al. 2017; Tabatabaenejad et al. 2015; Konings et al. 2014). At P-band (Sadeghi et al. 2017), such technology can be implemented based on the (Biomass monitoring mission for Carbon Assessment) BIOMASS polarimetric radar data (Carreiras et al. 2017). But this satellite has a low resolution (50 m) and the rare period of observation (25 days), these limitations will not allow measuring the spatial variations of soil moisture, within agricultural fields, continuously. The most promising approach that overcomes the existing limitations in the soil moisture remote sensing of individual farms is the use of lightweight UAVs, equipped with microwave radiometric or radar sensors. The possibilities of soil moisture remote sensing actively study using Global Positioning System (GPS) signals (Gamba et al. 2015; Alonso-Arroyo et al. 2015; Egido et al. 2014) and radiometric sensors (Dai et al. 2018; Acevo-Herrera et al. 2010; Shutko et al. 2006; Archer et al. 2004) on airborne platforms in the L-band. But moisture distribution in the arable layer cannot be directly retrieved using one frequency radar or radiometric measurements in the L-band. The impulse ultra-wideband (UWB) ground penetration radar (GPR) methods have proved their effectiveness in studying the geophysical properties of soils layered structure (Koyama et al. 2017; Ardekani and Lambot 2014; Daniels 2004). UWB GPR methods can be implemented on lightweight UAV platforms (Burr et al. 2018; García Fernández et al. 2018; Chandra and Tanzi et al. 2018). For the first time in (Wu et al. 2019) drone-borne, stepped-frequency continuous-wave (SFCW) radar in the P-band (500–700 MHz) for topsoil moisture mapping was presented. However, the measurement time at one frequency (dwell time) of modern compact SFCW radars is in the range of 100–200 μs (Šipoš and Gleich 2020; Planar R60 2020). The total number of frequency samples depends on the spectrum width of the radiated pulse and sweep duration in the time domain. (For example, at a UAV flight altitude of 100 m and the width of radiation spectrum of 1 GHz, in accordance with the 5th theorem (Kotelnikov 1933), at least 1334 frequency samples are required to describe the signal in the time domain from 0 ns to 667 ns (100 m). The whole process of the frequencies scanning will take about 0.13–0.27 s with a dwell time of 100–200 μs , respectively). Due to the finite time of frequencies scanning, significant changes in the reflective properties of the radar footprint area can occur as UAV moves. As a result, the coherence conditions between transmitted (received) signals at different

frequencies during scanning can be violated, which can increase the sidelobes level in a time-domain or almost destroy the signal.

In this regard, the choice of an optimal frequency band, as well as the finite set of the wave frequencies sufficient for remote sensing effective moisture and particularly soil moisture profiles are essential. In this work, an experimentally tested multi-frequency method for the remote sensing of vertical moisture profiles in the arable layer is suggested, which is suitable for use from UAVs.

2. Statement of the problem

Suppose that, similarly to the configuration (Wu et al. 2019, see Figure 1), remote sensing of the soil surface is carried out from airborne UAV using a microwave reflectometer and a nadir-looking broadband antenna. Remote sensing will be carried out at $n=6$ individual frequencies, f_j , in the band of amateur radio, which in many countries do not require licencing: $f_{j=1, \dots, 6} = (144 \text{ MHz}, 223 \text{ MHz}, 435 \text{ MHz}, 920 \text{ MHz}, 1.26 \text{ GHz}, 2.4 \text{ GHz})$. As a first step, the case of bare soil will be considered. Let the root-mean-square heights of the soil surface, h_r , satisfies the Rayleigh criterion $h_r < \lambda_{\min}/8$, λ_{\min} is the shortest wavelength of the

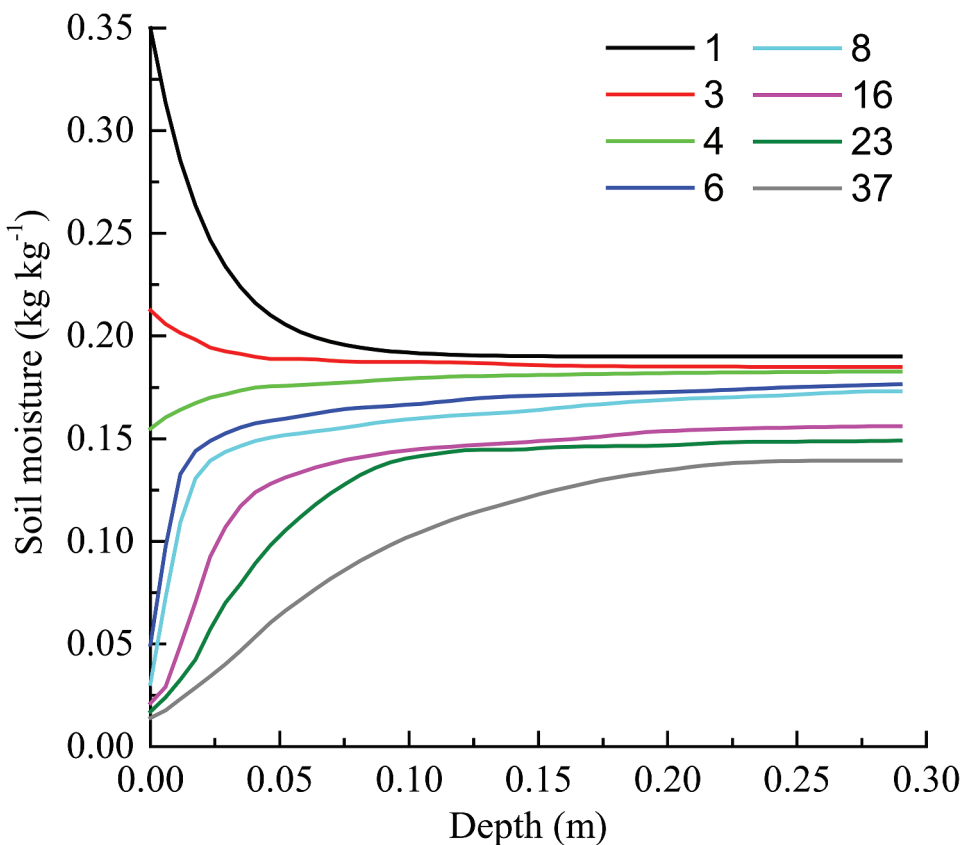


Figure 1. Moisture profiles in the arable layer between 1st and 37th day after irrigation.

emitted waves. Then, the reflection coefficients (power), R_j^m , measured at the frequencies of f_j , allow solving the inverse problem for maximum n -parameters (q_1, \dots, q_n):

$$(q_1, \dots, q_n) = \min \left\{ \sum_{j=1}^n \left| R_j^m - R_j^r(W^r(z, q_1, \dots, q_n), f_j) \right|^2 \right\} \quad (1)$$

where $W^r(z, q_1, \dots, q_n)$ is the parameterized arbitrary model function of soil moisture profile given in the abstract form, z is the vertical coordinate, $R_j^r(W^r(z, q_1, \dots, q_n), f_j)$ is reflection coefficient (power), calculated for the soil with moisture profile of $W^r(z, q_1, \dots, q_n)$ at a frequency of f_j . Soil type, texture and density will be assumed to be constant with depth.

2.1. Effective sensing depth

Following the formulated minimization problem (1) the thickness of topsoil, which is most essential for the formation of reflection coefficient, will be estimated for several reference moisture profiles. The reference moisture profiles $W^p(z)$ had been observed (Schmugge, Wilheit, and Gloersen 1976) at noon during 37 days (since 2 March 1971) after irrigation in one of the agricultural fields of the American Water Testing Labs in Phoenix (see Figure 1). The profile $p=1$ was not measured in (Schmugge, Wilheit, and Gloersen 1976) and was calculated in this paper as the result of two-dimensional interpolation of the moisture profiles between $p=3$ and $p=37$ days after irrigation. Let for each p^{th} soil moisture profile (see Figure 1) corresponding one value of effective soil moisture $W^r(z, q_1, \dots, q_n)W_{\text{eff}}^p$ can be found in the sense of the minimization problem (1), which in this case takes the form:

$$W_{\text{eff},j}^p = \min \left\{ \left| R_j^m - R_j^r(W_{\text{eff}}^p, f_j) \right|^2 \right\} \quad (2)$$

here R_j^m is the 'measured' reflection coefficients at the frequency of f_j , which calculates for the p^{th} reference moisture profile $W^p(z)$ (see Figure 1), $R_j^r(W_{\text{eff}}^p, f_j)$ is the modelled reflection coefficients, which calculates in the approximation of a dielectric homogeneous half-space with effective soil moisture value of W_{eff}^p . The reflection coefficients R_j^m for the inhomogeneous half-space are calculated by the iteration method (Brekhovskikh 1960, see paragraph 17.3) using complex permittivity model described in (Mironov et al. 2020). In accordance with the method (Brekhovskikh 1960, see paragraph 17.3), the reflection coefficient was calculated based on the iterative solution of the Riccati equation in integral form, while the stratified half-space ($0 > z > -0.3$ m) was subdivided into 1500 layers. The dielectric half-space for $z < -0.3$ m was considered homogeneous with complex permittivity $\varepsilon_s(z) = \varepsilon_s(z = -0.3$ m), where the subscripts 's' means a soil. At further calculations, the clay fraction and the dry density of the soil were set equal to 14% (U.S. Department of Agriculture (USDA) classification) and 10^3 kg m⁻³ (corresponds to often cultivated arable layer), respectively. The minimization problem (2) was solved using the Levenberg – Marquardt algorithm (Gill and Murray 1978). The retrieved values of effective soil moisture for different sensing frequencies f_j are shown in Figure 2 alongside with the soil surface moisture $W^p(z = 0\text{m})$ calculated for the reference profiles (see Figure 1) at a depth of $z = 0$ m. From the data are presented in Figure 2 it can be seen that retrieved

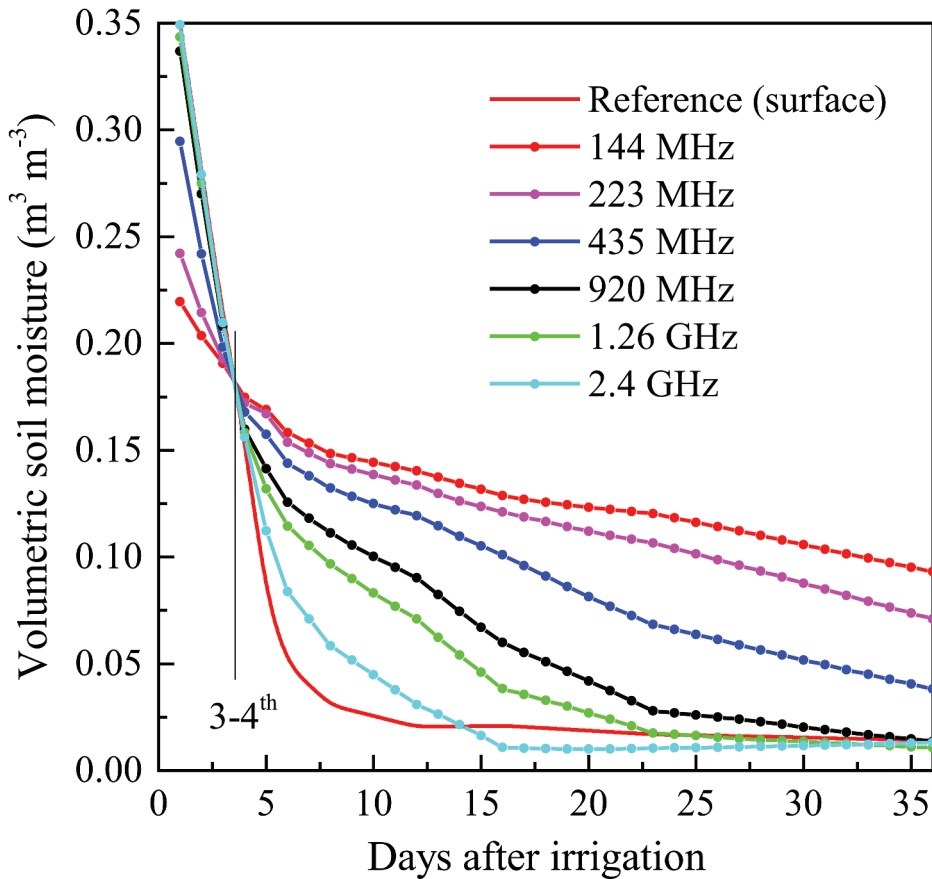


Figure 2. Retrieved values of effective soil moisture $W_{\text{eff},j}^p$ (colour curves with symbols) versus p^{th} day after irrigation at frequency of f_j . The solid red curve shows the soil surface moisture $W^p(z = 0\text{m})$ calculated for the reference profiles (see Figure 1) at a depth of $z = 0\text{m}$. Here the volumetric soil moisture was defined as a product of the weight moisture (see Figure 1) by the soil dry bulk density equal to 10^3 kg m^{-3} is plotted on the ordinate.

effective soil moisture at a frequency of 2.4 GHz with a standard deviation of less than $0.013\text{ m}^3\text{ m}^{-3}$ corresponds to the surface soil moisture (at $z = 0\text{m}$). Until the 4th day after an irrigation (when the surface soil moisture exceeds $0.15\text{ m}^3\text{ m}^{-3}$, see Figures 1 and 2), the soil moistures retrieved in the frequency range from 920 MHz to 2.4 GHz practically coincide. It seems likely that for the considered type of soil when the surface moisture exceeded $0.15\text{ m}^3\text{ m}^{-3}$, the possibility of obtaining information about moisture distribution with depth can be provided by sensing frequencies 435 MHz and lower. As expected, the effective soil moisture, retrieved in the frequency range from 144 MHz to 435 MHz (see Figure 2) has more information about moisture distribution with depth before and after 4th day after irrigation. The observed differences between the reference moisture at the soil surface $W^p(z = 0\text{m})$ (see Figure 2, solid red curve) and the retrieved effective soil moisture $W_{\text{eff},j}^p$ are associated with the different thicknesses of topsoil, within which waves

reflection are mostly formed. At each frequency of f_j the thickness (or effective sensing depth) d_j of the topsoil can be estimated using the nonlinear equation:

$$\frac{1}{d_j} \int_0^{d_j} dz W^p(z) = W_{\text{eff},j}^p \quad (3)$$

where the left side of the Equation (3) is average moisture value in the topsoil thickness of d_j , $W^p(z)$ and $W_{\text{eff},j}^p$ are determined for each p^{th} day after irrigation in Figure 1 and Figure 2, respectively. The results of the calculations are shown in Figure 3. Indeed, as can be seen from Figure 3, the sensing depth at a frequency of 2.4 GHz does not exceed $0.88 \cdot 10^{-3}$ m, thereby the retrieved value of effective moisture on this frequency practically coincides with the surface soil moisture (see Figure 2). The maximum sensing depth reaches 0.211 m at a frequency of 144 MHz (see Figure 3). The sensing depth in L-band (1.26 GHz) reaches about 0.02 m (see Figure 3), which is in good agreement with the literature data (Escorihuela et al. 2010; Choudhury et al. 1979). The sensing depth depends not only on frequency but also on the shape of moisture profiles (see Figure 3 and Figure 1 for the corresponding days after

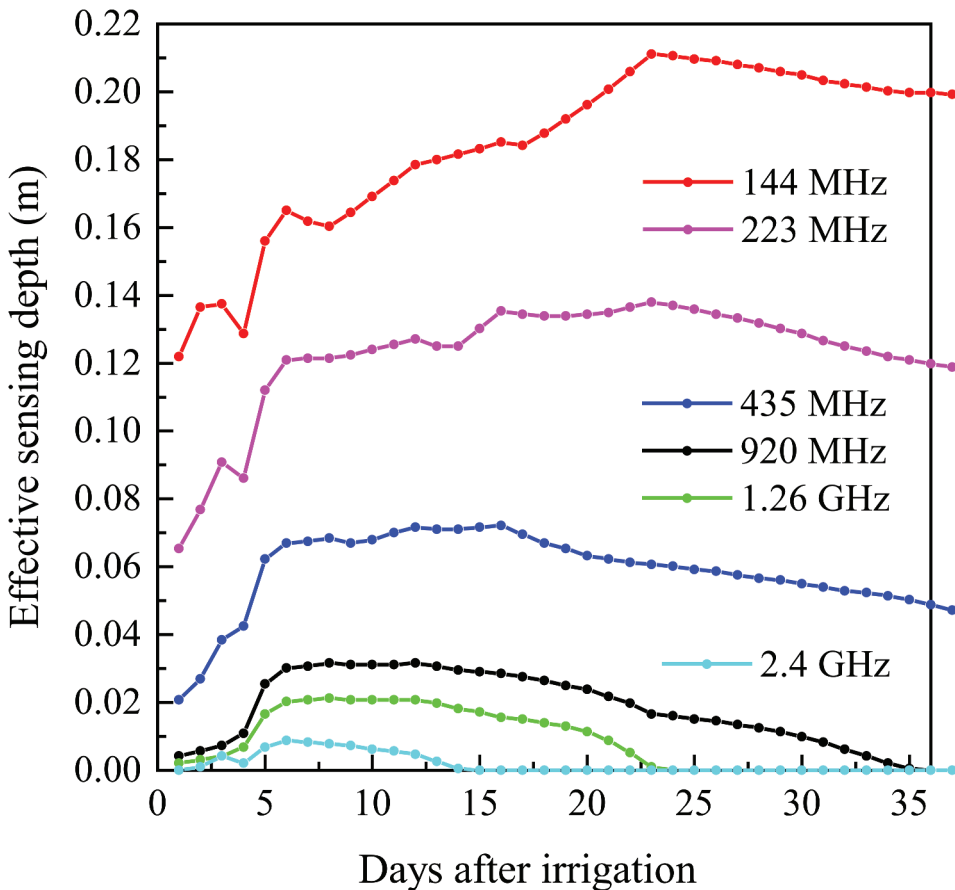


Figure 3. The thickness of topsoil, the average moisture in which is equal to the effective soil moisture (see Figure 2).

irrigation). The sensing depth reaches a maximum from 6th to 25th day, after irrigation when the moisture profiles (or which is the same, the refractive index) had a maximal gradient in the layer thickness of d_j (compare Figures 1 and 3). Indeed, as shown in (Brekhovskikh 1960, see Equation 15.22), for the linear model of refractive index profile versus depth, the reflection coefficient is directly proportional to the gradient of refractive index at the soil surface. A twofold increase wave frequency from 144 MHz (sensing depth is 0.138 m) to 223 MHz (0.211 m) practically leads to the same retrieved value of effective soil moisture (compare Figures 2 and 3). Only after 18th day after irrigation (see Figure 2), the retrieved values of effective soil moisture on frequencies of 435 MHz and 144 MHz differs more than $0.04 \text{ m}^3 \text{ m}^{-3}$ (target error of soil moisture measurement for many satellite systems (Entekhabi et al. 2014)). Our analysis shows frequencies no less than 223 MHz may be selected as the lower limit in the set of wave frequencies if a long dry period not observed and the purpose of remote sensing is to retrieve soil moisture profiles in the arable layer.

2.2. The set of frequencies for the retrieval of moisture profiles in the arable layer

Let us determine the minimum set of frequencies from 223 MHz to 2.4 GHz (in the band of amateur radio), which are sufficient for retrieving with acceptable accuracy of soil moisture profiles (see Figure 1) while solving the inverse problem (1). By virtue of the limited number of multi-frequency observations, to theoretical describe the experimental moisture profiles (see Figure 1), we take advantage of the simplified solution of the equation of vertical soil moisture transfer (Sadeghi et al. 2017):

$$W^r(z, W_0, W_\infty, \alpha) = W_\infty + (W_0 - W_\infty)\exp(z/\alpha) \quad (4)$$

where W_0 is the surface soil moisture, W_∞ is the moisture outside of arable layer at $z \rightarrow -\infty$, and α is the effective thickness of the capillary edge. As an example, in Figure 4, for 1st, 10th and 35th day after irrigation, the soil moisture profiles $W^r(z, W_0, W_\infty, \alpha)$, retrieved during the solution of the inverse problem (1) for the different sets of wave frequencies, are presented. Based on a qualitative analysis of the data presented in Figure 4, we can do the following conclusions. Firstly, adding a frequency of 223 MHz to a frequency of 435 MHz does not significantly improve the accuracy of retrieving profiles (for the given soil texture and reference moisture profiles). Secondly, removal a frequency of 2.4 GHz from the frequency sets (in the presence of frequency 1.26 GHz) does not lead to the significant increase of the error of soil moisture profiles retrieval (see Figure 4). Thirdly, removal a frequency of 435 MHz from the frequency sets (in the absence of frequency 223 MHz) leads to the significant increase of the error of soil moisture profiles retrieval. The calculations also showed that using frequencies only in MHz-band (excluding 1.26 GHz and 2.4 GHz) lead to overestimation of the soil moisture retrieving at the surface on $0.06 \text{ m}^3 \text{ m}^{-3}$. The conducting theoretical calculations show that the set of three frequencies in P- and L-bands of amateur radio (1.26 GHz, 920 MHz, 435 MHz) is sufficient for the retrieving of exponential moisture profiles in the arable layer. In the next section, the experiment of soil moisture profiles remote sensing based on the three-frequency measurements of the reflection coefficient is described.

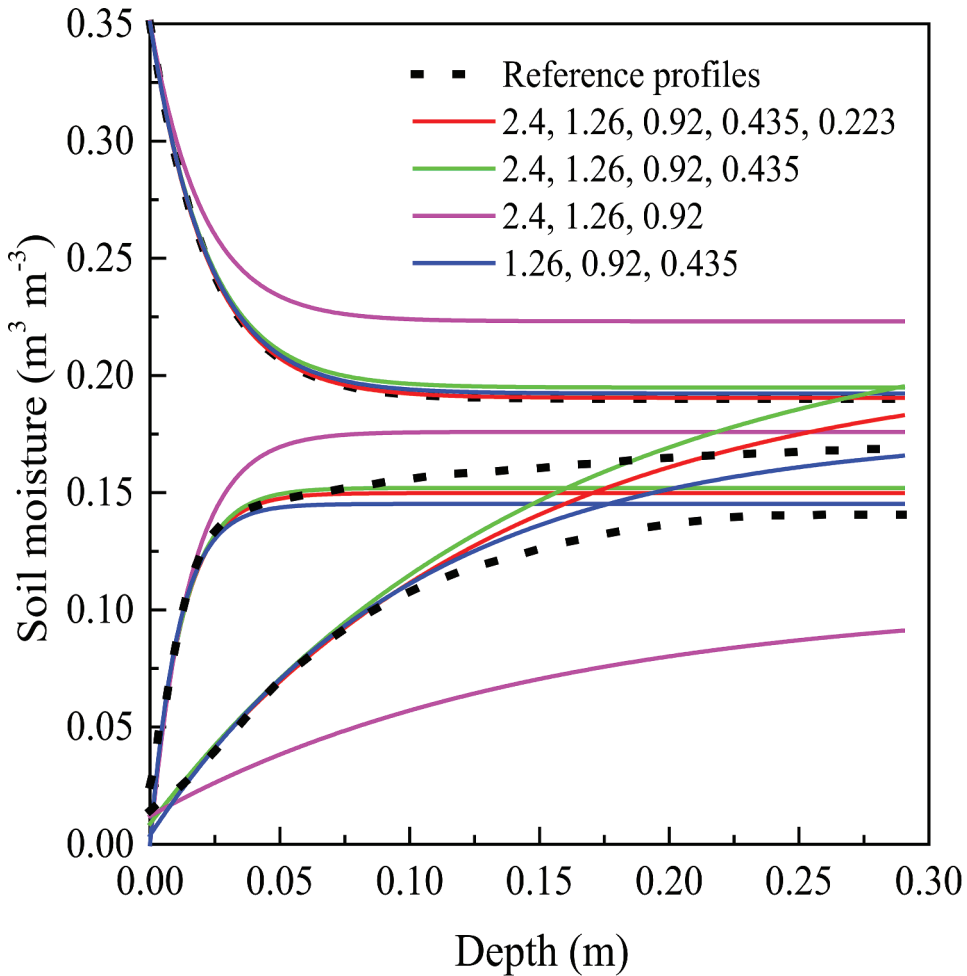


Figure 4. Reference (see Figure 1) and retrieved soil moisture profiles for various set of frequencies for 1st, 10th and 35th day after irrigation. The frequency values in the figure are indicated in GHz.

3. Experiment description

From 18 July to 8 August 2019, reflection coefficients were measured on the test plot (3 m by 3 m in size) of an agricultural field being under steam, located at 56°05' N, 92°40' E in the area of Minino village, Krasnoyarsk region, the Russian Federation. The soil surface of test plot was smoothed out to reduce the impact of soil surface roughness. Root-mean-square heights of the soil surface were in the range from $5.7 \cdot 10^{-3}$ to $8.2 \cdot 10^{-3}$ m. Average dry bulk density and clay content in the topsoil thickness of about 25 cm were $1.16 \cdot 10^3$ kg m⁻³ and about 26%, respectively. The vertical profiles of volumetric moisture in the arable layer were measured layer by layer with a GS3 sensor (Decagon, USA) with an error no worse than 0.04 m³ m⁻³. Reflection coefficients were measured using the log-periodic (Kent Electronics, U.S., $S_{11} < 14$ dB in the range from about 462 to 978 MHz) and broadband horn P6-59 (KRET, Nizhny Novgorod, Russia, $S_{11} < 14$ dB in the range from about 1 to 17 GHz) antennas, respectively. Antennas were located at a height of about 1.4 m above

the soil surface. Reflection coefficients (power) were measured by a radio impulse method using calibration methodology (relative to a metal screen) follow the article (Serbin and Or 2004). Radio impulses (about 300 MHz spectrum width) at the central frequencies of f_j (see Table 1) were synthesized using the approach (Robinson, Weir, and Young 1974), based on the spectral measurement of S_{12} transmission parameter. The S_{12} transmission parameter was measured by Agilent N9918A FieldFox vector network analyser to the terminals of which transmitter and receiver antennas were connected. Before the measurements, the vector network analyser switched on for about 30 minutes, after that, it was calibrated using a standard mechanical calibrator (Full 2-port CalKit, 85518A, Type-N-50 Ohm). This calibration provides an amplitude measurement with an accuracy of 0.35 dB in the amplitudes range of receives signals from -20 to 0 dB at frequencies <9 GHz.

The values of reflection coefficients were measured at the central frequencies (1.26 GHz, 796 MHz and 641 MHz) of radio impulses (see Table 1). Using the measured reflection coefficients at three frequencies (see Table 1), the inverse problem (1) at $n=3$, which reduces functional F to a minimum using the model profile (4) was solved. The minimization problem (1) was solved by means of the Levenberg – Marquardt algorithm (Gill and Murray 1978). This algorithm ensured the convergence of the problem to a global minimum in the meaning of minimum residual norm between the measured and calculated values of reflection coefficients. Retrieved and measured soil moisture profiles for several days are shown in Figure 5. Correlation between the retrieved and measured moisture into the topsoil thickness of 0.15 m is shown in Figure 6.

4. Results and discussion

The proposed method with high accuracy allows retrieving the moisture profiles in the arable layer based on the measurements of reflection coefficient at three frequencies. Herewith, the soil surface roughness ($6\text{--}8 \cdot 10^{-3}$ m) of the test plot did not have a significant effect on the error of soil moisture retrieval (see Figures 5 and 6) in the frequency band from 641 MHz to 1.26 GHz. The root-mean-square error (RMSE) and determination coefficient (R^2) between the retrieved and measured soil moisture values were appeared to be $0.033 \text{ m}^3 \text{ m}^{-3}$ and 0.79, respectively (see Figure 6). The highest dispersion observes at the depths of more than 0.12–0.14 m (see Figure 5), where soil moisture exceeds about $0.2 \text{ m}^3 \text{ m}^{-3}$ (see Figure 6). On the one hand, at these depths and deeper, the measured soil moisture profiles (see Figure 5) worse describes by the exponential model (4). On the other hand, with increasing soil moisture, the depth of wave penetration decreases. As a result, it is necessary to use a more complicated model of soil moisture profiles than (4) for the retrieval with higher accuracy of soil moisture deeper than 0.12–0.14 m. Such

Table 1. Absolute values of reflection coefficients measured during the experiment.

| f_j^* (GHz) | Date | | | | | | |
|---------------|---------|---------|---------|---------|----------|----------|----------|
| | 18 July | 22 July | 29 July | 30 July | 5 August | 7 August | 8 August |
| 1.260 | 0.247 | 0.519 | 0.417 | 0.380 | 0.266 | 0.258 | 0.316 |
| 0.796 | 0.331 | 0.541 | 0.438 | 0.425 | 0.314 | 0.291 | 0.295 |
| 0.641 | 0.382 | 0.577 | 0.496 | 0.487 | 0.392 | 0.359 | 0.336 |

*The choice of the centre frequencies 796 MHz and 641 MHz were determined by the limited bandwidth of the log-periodic antenna and duration of the emitted radio impulses. These conditions did not allow forming radio impulses on the central frequencies 920 MHz and 435 MHz.

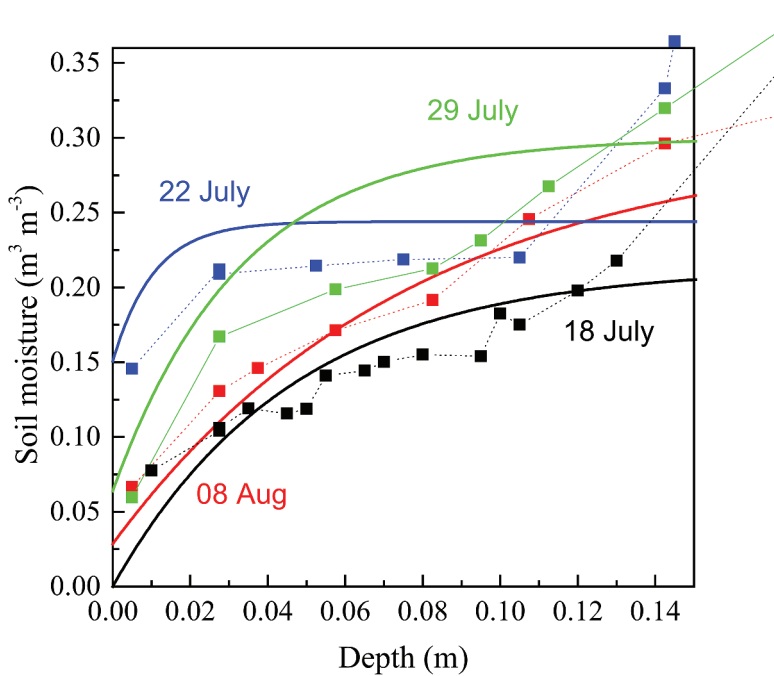


Figure 5. Retrieved (solid lines) and measured (symbols) soil moisture profiles on 22 and 29 July (two cases with the most significant errors) and on 18 July and 8 August (typical cases).

a profile model (with the number of retrieved parameters more than three) will require additional measurements of reflection coefficients. However, the use frequencies of 144 MHz and 233 MHz from the amateur radio band will require bulky antenna structures, which are not suitable for placement on ultralight UAVs. In this regard, the use of impulse UWB GPR technologies seems to be the most promising for the formulation of inverse multi-parametric problems in the field of the remote sensing of soil moisture profiles from ultralight UAV platforms.

The results of theoretical modelling show it is necessary to use at least one frequency from the GHz-band for retrieving of moisture at the soil surface with high accuracy. Theoretical modelling also shows that, based on the measurements of effective soil moisture at different frequencies, it is possible to determine the moment in time when the sign of gradient in the moisture profile of arable layer changes (3rd and 4th days after irrigation, see Figure 2). If retrieved on different frequencies values of effective soil moisture are close to each other, it can be said that there is no moisture profile and the soil is moistened uniformly with depth (see Figure 2, between 3rd and 4th days).

5. Conclusions

In contrast to the retrieval on fixed frequencies of effective moisture values, which are difficult to correlate with a specific thickness of topsoil, the most justified is the direct retrieval of moisture profiles in the arable layer. In this paper, a remote method for the measuring of moisture profiles in the arable layer thickness of 0.15 m with an error

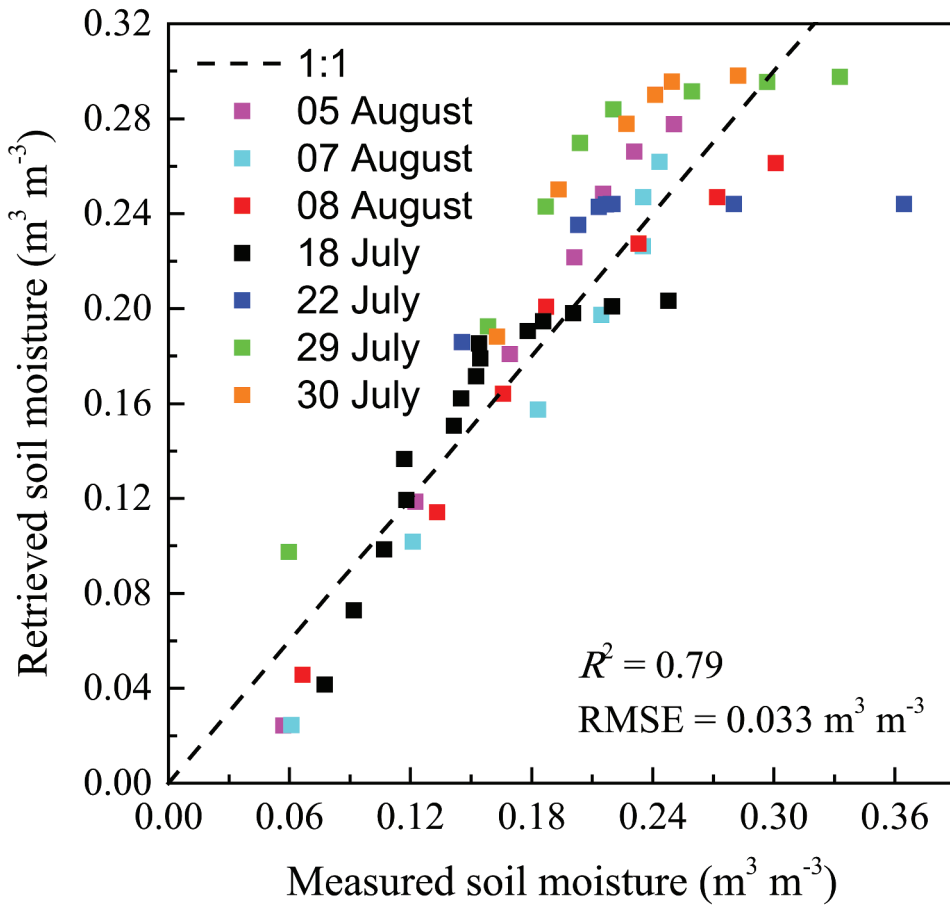


Figure 6. Retrieved soil moisture versus measured one in the topsoil thickness of 0.15 m.

acceptable for practice ($0.033 \text{ m}^3 \text{m}^{-3}$) is proposed and experimentally tested. The proposed method is based on the measurements of reflection coefficients at three frequencies: 1.26 GHz, 796 MHz and 641 MHz. The relative compactness of antennas in this frequency range allows them to implement on lightweight UAVs. Improving the accuracy of soil moisture profiles retrieval can be achieved by the measurements of reflection coefficients using a more substantial amount of frequencies (than three) within the band from 435 MHz to 1.26 GHz. A larger number of measurements on different frequencies will allow solving a multi-parameter inverse problem with using a more complicated soil moisture profile (than the exponential). In this case, the undeniable advantage is using UWB impulse signals, the spectrum of which concentrates in the MHz-band. A particular technical issue that needs to be studied is the choice between the time or spectral domain method of generating and receiving UWB signals. UWB generators and stroboscopic receivers in the time domain have high speed. However, the shape and spectrum of generated impulses are strictly defined by each device, and similar devices (GPR) are expensive. The generation and receiving of UWB signals in the spectral domain by compact vector network analysers have adaptive flexibility of digital signal processing and low cost. However, they have a low

speed of operation. The optimal minimum set of frequencies (similar to that was proposed in this work) on which reflection coefficients measure, will allow increasing the speed of whole measurement process with using relatively slow and cheap compacted vector network analysers. At the same time, it is necessary to clarify the choice of the optimal set of frequencies used for retrieving of soil moisture profiles depending on soil texture and density, soil surface roughness, biomass and kind of crops. From our point of view, in the future, such adaptive methods will allow introducing low-cost technology for the remote sensing of soil moisture profiles for individual farms from the board of lightweight UAVs.

Disclosure statement

No potential conflict of interest was reported by the author.

Funding

This work was supported by the Russian Foundation for Basic Research (grant No. 18-05-00405) in part of the sensing depth investigation and retrieving soil moisture. The method of the formation of radio impulses was created in part of SB RAS project No. 0356-2019-0004

References

- Acevo-Herrera, R., A. Aguasca, X. Bosch-Lluis, A. Camps, J. Martínez-Fernández, N. Sánchez-Martín, C. Pérez-Gutiérrez et al. 2010. "Design and First Results of an UAV-Borne L-Band Radiometer for Multiple Monitoring Purposes." *Remote Sensing* 2 (7): 1662–1679. doi:10.3390/rs2071662.
- Alonso-Arroyo, A., N. Sanchez, M. Pablos, A. Gonzalez-Zamora, J. Martinez-Fernandez, M. Vall-Ilosera, D. Pascual. 2015. "An Airborne GNSS-R Field Experiment over a Vineyard for Soil Moisture Estimation and Monitoring." IEEE International Geoscience and Remote Sensing Symposium, Milan:4761–4764.
- Archer, F., A.M. Shutko, T.L. Coleman, A. Haldin, E. Novichikhin, I. Sidorov. 2004. "Introduction, Overview, and Status of the Microwave Autonomous Copter System (MACS)." IEEE International Geoscience and Remote Sensing Symposium, Anchorage. 5: 3574–3576.
- Ardekani, M. R., and S. Lambot. 2014. "Full-Wave Calibration of Time- and Frequency-Domain Ground-Penetrating Radar in Far-Field Conditions." *IEEE Transactions on Geoscience and Remote Sensing* 52 (1): 664–678. doi:10.1109/TGRS.2013.2243458.
- Brekhovskikh, L. M. 1960. *Waves in Layered Media*, 574. New York, NY, USA: Academic Press.
- Burr, R., M. Schartel, P. Schmidt, W. Mayer, T. Walter, C. Waldschmidt. 2018. "Design and Implementation of a FMCW GPR for UAV-based Mine Detection." IEEE MTT-S International Conference on Microwaves for Intelligent Mobility, Munich: 1–4.
- Candiago, S., F. Remondino, M. De Giglio, M. Dubbini, M. Gattelli. 2015. "Evaluating Multispectral Images and Vegetation Indices for Precision Farming Applications from UAV Images." *Remote Sensing* 7 (4): 4026–4047. doi:10.3390/rs70404026.
- Carreiras, J. M. B., S. Quegan, T. Leo, D. Ho Tong Minh, S. S. Saatchi, N. Carvalhais, M. Reichstein, and K. Scipal. 2017. "Coverage of High BIOMASS Forests by the ESA BIOMASS Mission under Defense Restrictions." *Remote Sensing of Environment* 196: 154–162. doi:10.1016/j.rse.2017.05.003.
- Chandra, M., T. J. Tanzi. 2018. "Drone-borne GPR Design: Propagation Issues." *Comptes Rendus Physique* 19 (1–2): 72–84. doi:10.1016/j.crhy.2018.01.002.
- Choudhury, B., T. Schumge, A. Chang, and R. Newton. 1979. "Effect of Surface Roughness on the Microwave Emission from Soils." *Journal of Geophysical Research* 84 (C9): 5699–5706. doi:10.1029/JC084iC09p05699.

- Dai, E., A. Venkatasubramony, A. Gasiewski, M. Stachura, and J. Elston. 2018. "High Spatial Soil Moisture Mapping Using Small Unmanned Aerial System." IEEE International Geoscience and Remote Sensing Symposium, Valencia: 6496–6499.
- Daniels, D. 2004. *Ground Penetrating Radar*, 984. 2nd ed. Institution of Electrical Engineer, London, U. K.
- Egido, A., S. Paloscia, E. Motte, L. Guerriero, N. Pierdicca, M. Caparrini, E. Santi et al. 2014. "Airborne GNSS-R Soil Moisture and above Ground Biomass Observations." *The IEEE Journal of Selected Topics in Applied Earth Observations and Remote Sensing* 7 (5): 1522–1532. doi:10.1109/JSTARS.2014.2322854.
- Entekhabi, D., S. Yueh, P. O'Neill, and K. Kellogg. 2014. *SMAP Handbook*, 400–1567. Pasadena, CA, USA: Jet Propulsion Lab.
- Escorihuela, M., A. Chanzy, J. Wigneron, and Y. Kerr. 2010. "Effective Soil Sampling Depth of the L-band Radiometry: A Case Study." *Remote Sensing of Environment* 114 (5): 995–1001. doi:10.1016/j.rse.2009.12.011.
- Gamba, M., G. Marucco, M. Pini, S. Ugazio, E. Falletti, L. Lo Presti. 2015. "Prototyping a GNSS-Based Passive Radar for UAVs: An Instrument to Classify the Water Content Feature of Lands." *Sensors* 15 (11): 28287–28313. doi:10.3390/s151128287.
- García Fernández, M., Y. Alvarez Lopez, A. Arboleya Arboleya, B. Gonzalez Valdes, Y. Rodriguez Vaqueiro, F. Las-Heras Andres, A. Pino Garcia, et al. 2018. "Synthetic Aperture Radar Imaging System for Landmine Detection Using a Ground Penetrating Radar on Board a Unmanned Aerial Vehicle". *IEEE Access* 6: 45100–45112. doi:10.1109/ACCESS.2018.2863572.
- Gill, P. E., and W. Murray. 1978. "Algorithms for Nonlinear Least-Squares Problem." *SIAM Journal on Numerical Analysis* 15 (5): 977–992. doi:10.1137/0715063.
- Haboudane, D., J. R. Miller, E. Pattey, P. J. Zarco-Tejada, I. B. Strachan. 2004. "Hyperspectral Vegetation Indices and Novel Algorithms for Predicting Green LAI of Crop Canopies: Modeling and Validation in the Context of Precision Agriculture." *Remote Sensing of Environment* 90 (3): 337–352. doi:10.1016/j.rse.2003.12.013.
- Konings, A. G., D. Entekhabi, M. Moghaddam, and S. S. Saatchi. 2014. "The Effect of Variable Soil Moisture Profiles on the P-Band Backscatter." *IEEE Transactions on Geoscience and Remote Sensing* 52 (10): 6315–6325. doi:10.1109/TGRS.2013.2296035.
- Kotelnikov, V. A. 1933. "On the Capacity of the 'Ether' and Cables in Electrical Communication." Proc. 1st All-Union Conf. Technological Reconstruction of the Commun. Sector and Low-Current Eng, Moscow. http://thesoundmanifesto.co.uk/papers/TransmissionCapacity_Kotelnikov_1933.pdf
- Koyama, C. N., H. Liu, K. Takahashi, M. Shimada, M. Watanabe, T. Khuut, M. Sato, et al. 2017. "In-Situ Measurement of Soil Permittivity at Various Depths for the Calibration and Validation of Low-Frequency SAR Soil Moisture Models by Using GPR." *Remote Sensing* 9 (580). doi:10.3390/rs9060580.
- Mironov, V. L., A. Yu., I. Yu., I. Lukin, and P. Molostov. 2020. "A Dielectric Model of Thawed and Frozen Arctic Soils considering Frequency, Temperature, Texture, and Dry Density." *International Journal of Remote Sensing* 41 (10): 3845–3865. doi:10.1080/01431161.2019.1708506.
- Planar R60, 2020. Copper Mountain Technologies, Indianapolis, USA, . <https://coppermountaintech.com/vna/r60-1-port/>
- Robinson, L. A., W. B. Weir, and L. Young. 1974. "Location and Recognition of Discontinuities in Dielectric Media Using Synthetic RF Pulses." *Proceedings of the IEEE* 62 (1): 36–44. doi:10.1109/PROC.1974.9383.
- Sadeghi, M., A. Tabatabaenejad, M. Tuller, M. Moghaddam, and S. B. Jones. 2017. "Advancing NASA's AirMOSS P-Band Radar Root Zone Soil Moisture Retrieval Algorithm via Incorporation of Richards' Equation." *Remote Sensing* 9 (1): 1–17.
- Schmugge, T. 1978. "Remote Sensing of Surface Soil Moisture." *Journal of Applied Meteorology* 17 (10): 1549–1557. doi:10.1175/1520-0450(1978)017<1549:RSOSSM>2.0.CO;2.
- Schmugge, T., W. Wilheit Jr., and W. P. Gloersen. 1976. "Remote Sensing of Soil Moisture with Microwave radiometers-II." NASA technical note D-8321: 34.

- Serbin, G., and D. Or. 2004. "Ground-penetrating Radar Measurement of Soil Water Content Dynamics Using a Suspended Horn Antenna." *IEEE Transactions on Geoscience and Remote Sensing* 42 (8): 1695–1705. doi:[10.1109/TGRS.2004.831693](https://doi.org/10.1109/TGRS.2004.831693).
- Shutko, A. M. 1982. "Microwave Radiometry of Lands under Natural and Artificial Moistening." *IEEE Transactions on Geoscience and Remote Sensing*, no. 1: 18–26. doi:[10.1109/TGRS.1982.4307514](https://doi.org/10.1109/TGRS.1982.4307514).
- Shutko, A. M., S. P. Golovachev, E. P. Novichikhin, A. A. Haldin, V. F. Krapivin, I. A. Sidorov, T. L. Coleman, T. Dachev, R. Haarbrink, A. D. Krissilov, A. D. Archer, W. Tadesse. 2006. "Teaching and Conducting Scientific Research: An Experience in Joint USA-Russia-Bulgaria-Holland-Ukraine International Collaboration Between." *IEEE MicroRad*, San Juan: 82-86.
- Šipoš, D., and D. Gleich. 2020. "A Lightweight and Low-Power UAV-Borne Ground Penetrating Radar Design for Landmine Detection." *Sensors* 22 (2234). doi:[10.3390/s20082234](https://doi.org/10.3390/s20082234).
- Tabatabaenejad, A., M. Burgin, X. Duan, and M. Moghaddam. 2015. "P-Band Radar Retrieval of Subsurface Soil Moisture Profile as a Second Order Polynomial: First AirMOSS Results." *IEEE Transaction on Geoscience and Remote Sensing* 53 (2): 645–658. doi:[10.1109/TGRS.2014.2326839](https://doi.org/10.1109/TGRS.2014.2326839).
- Ulaby, F., and D. Long. 2015. *Microwave Radar and Radiometric Remote Sensing*, 1014. Norwood, MA: Artech House.
- Wu, K., G. A. Rodriguez, M. Zajc, E. Jacquemin, M. Clément, A. De Coster, S. Lambot, et al. 2019. "A New Drone-borne GPR for Soil Moisture Mapping". *Remote Sensing of Environment* 235: 111456. doi:[10.1016/j.rse.2019.111456](https://doi.org/10.1016/j.rse.2019.111456).